

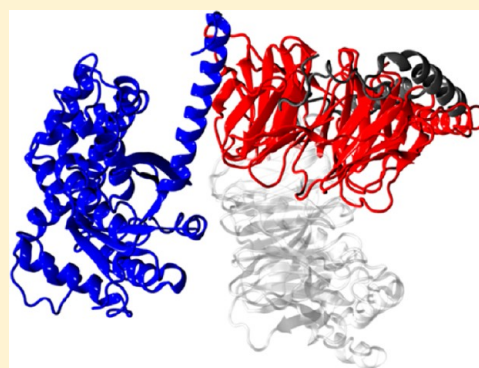
# Dissociation of Membrane-Anchored Heterotrimeric G-Protein Induced by $G_\alpha$ Subunit Binding to GTP

Maxime Louet, Landry Charlier, Jean Martinez, and Nicolas Floquet\*

Institut des Biomolécules Max Mousseron (IBMM), CNRS UMR5247, Université Montpellier 1, Université Montpellier 2, Faculté de Pharmacie, 15 av. Charles Flahault, BP 14491, 34093 Montpellier Cedex 05, France

## S Supporting Information

**ABSTRACT:** Heterotrimeric G-proteins' activation on the intracellular side of the cell membrane is initiated by stimulation of the G-Protein Coupled Receptors (GPCRs) extra-cellular part. This two-step activation mechanism includes (1) an exchange between GDP and GTP molecules in the  $G_\alpha$  subunit and (2) a dissociation of the whole  $G_{\alpha\beta\gamma}$  complex into two membrane-anchored blocks, namely the isolated  $G_\alpha$  and  $G_{\beta\gamma}$  subunits. Although X-ray data are available for both inactive  $G_{\alpha\beta\gamma}$ :GDP and active  $G_\alpha$ :GTP complexes, intermediate steps involved in the molecular mechanism of the dissociation have not yet been addressed at the molecular level. In this study, we first built a membrane-anchored intermediate  $G_{\alpha\beta\gamma}$ :GTP complex. This model was then equilibrated by molecular dynamics simulations before the Targeted Molecular Dynamics (TMD) technique was used to force the  $G_\alpha$  subunit to evolve from its inactive (GDP-bound) to its active (GTP-bound) conformations, as described by available X-ray data. The TMD constraint was applied only to the  $G_\alpha$  subunit so that the resulting global rearrangements acting on the whole  $G_{\alpha\beta\gamma}$ :GTP heterotrimer could be analyzed. We showed how these mainly local conformational changes of  $G_\alpha$  could initiate large domain:domain motions of the whole complex, the  $G_{\beta\gamma}$  behaving as an almost quasi-rigid block. This separation of the two  $G_\alpha$ :GTP and  $G_{\beta\gamma}$  subunits required the loss of several interactions at the  $G_\alpha$ : $G_{\beta\gamma}$  interface that were reported. This study provided an atomistic view of the crucial intermediate step of the G-proteins activation, e.g., the dissociation, that could hardly be elucidated by the experiment.



## INTRODUCTION

G-Protein Coupled Receptors (GPCRs) form a large family of mammals' transmembrane proteins that are targeted by almost 40% of today's marketed drugs.<sup>1</sup> After GPCR stimulation on the extra-cellular side of the cell membrane, G-proteins act as the first protagonist of the subsequent intracellular signal transduction. G-proteins are made of three different protein subunits, namely,  $G_\alpha$ ,  $G_\beta$ , and  $G_\gamma$ .  $G_\alpha$  and  $G_\gamma$  both being anchored to the biological membrane through lipid-modified residues. As compared to small G-proteins, the  $G_\alpha$  subunit of heterotrimeric G-proteins is subdivided into two tightly bound «ras-like» and helical subdomains (see Figure 1A), at the interface of which lies a Guanosine Di-Phosphate (GDP). Activation of G-proteins begins with an exchange between this GDP and a GTP molecule at this interdomain interface of  $G_\alpha$ . This exchange is thought to be promoted by the conformational rearrangements of the whole GPCR:G-protein complex that result from ligand binding into the dedicated crevice of the receptor. Such an exchange also exists in the absence of the receptor, at a lower level.<sup>2</sup>

Many X-ray structures are available in the Protein Data Bank that describe the  $G_\alpha$  subunit complexed to GDP or diverse GTP analogues. Together, these structural data first show that GDP and GTP molecules both bind to almost the same pocket and interact with almost all the same key residues. However,

only a difference of one additional phosphate group in the GTP molecule appears to be sufficient to promote some local conformational rearrangements of the  $G_\alpha$  subunit (see Figure 1B)<sup>3</sup> and subsequently leads to the dissociation of the larger protein:protein complex. These local structural changes (see Figure 1A) include mainly the formation of two additional helix turns in the switches II and IV regions and a loop motion of the switch III region that comes closer to the GTP.

Unfortunately, available X-ray data only describe the initial ( $G_{\alpha\beta\gamma}$ :GDP),<sup>4,5</sup> the nucleotide empty complex ( $G_{\alpha\beta\gamma}$ ),<sup>6</sup> and the final states ( $G_\alpha$ :GTP +  $G_{\beta\gamma}$ )<sup>7–9</sup> of this activation mechanism, the possible intermediate conformations/motions of the protein still remaining unsolved. Among other important questions, it can still be debated whether the observed local conformational changes around the GTP ligand are directly due to the GDP:GTP exchange in the  $G_\alpha$  subunit, or if they could result from dissociation of the whole heterotrimer. X-ray structures of the isolated GDP-bound  $G_\alpha$  subunit suggested that the switch II region appears to be much more flexible,<sup>2</sup> arguing for a direct role of the GTP in the local structural rearrangements. These rearrangements are observed in quite a number of X-ray structures available for the isolated  $G_\alpha$ :GTP

Received: August 9, 2012

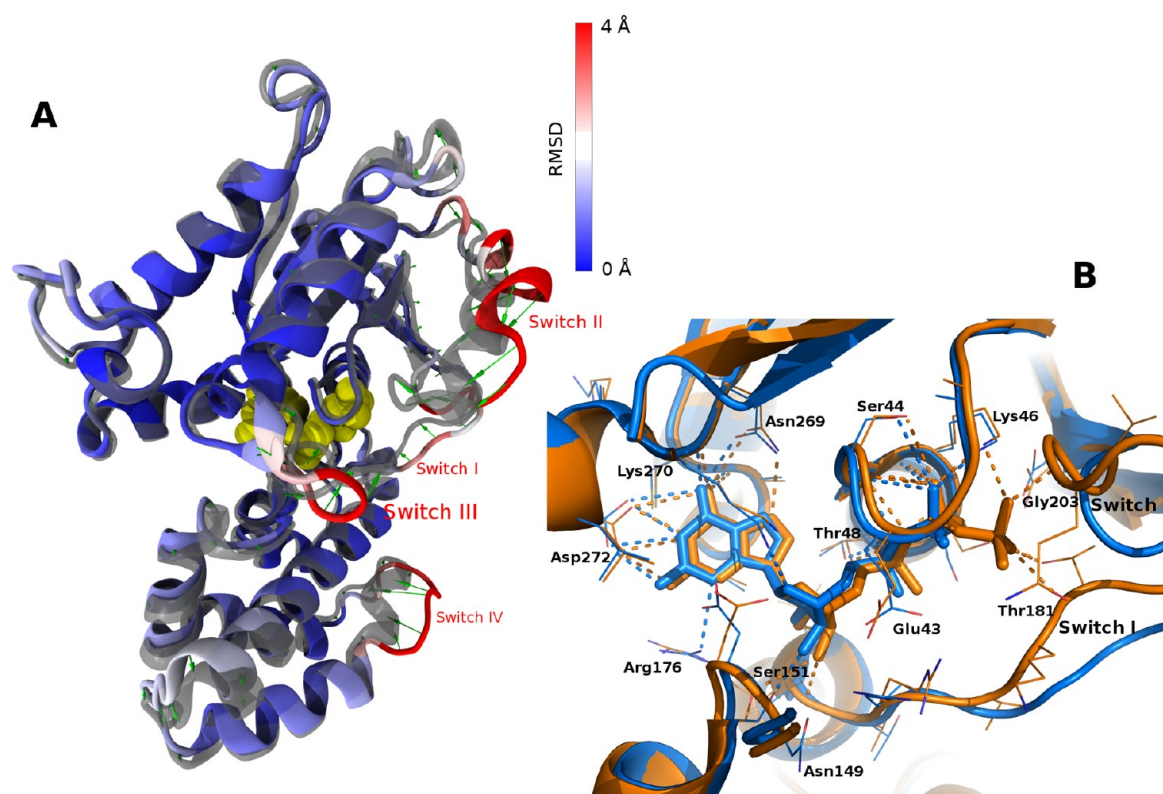


**Figure 1.** (A) Structural rearrangements of the  $G_\alpha$  subunit between GDP and GTP bound conformations (opaque and transparent ribbons, respectively), indicated by green arrows. The color scale corresponds to the per-residue RMSD computed between the two structures. The GDP molecule was reported as yellow spheres. (B) Local interactions of GDP (blue) and GTP (orange) in the binding pocket of  $G_\alpha$  showing a high degree of similarity outside the switch regions.

subunit. Finally, orientations of both switches I and II in the recently described GPCR: $G_{\alpha\beta\gamma}$  complex indicate that these conformational changes are not resulting from GDP release only.<sup>6</sup> In agreement, structural rearrangements that occur in the  $G_\alpha$  subunit can be confidently associated to GTP binding.

In this study, we have addressed at the molecular level the possible implication of these experimentally observed local conformational changes of the  $G_\alpha$  subunit in the putative dissociation process of the whole  $G_{\alpha\beta\gamma}$  heterotrimer.

## MATERIAL AND METHODS

**Equilibration of the Initial Model.** The  $G_i$  heterotrimer (PDB code: 1GP2)<sup>10</sup> was used as a starting conformation for an initial 90 ns molecular dynamics simulation, performed with NAMD<sup>11</sup> and the CHARMM27 force field<sup>12</sup> with CMAP corrections.<sup>13</sup> First, lacking residues were added at the N- and C-ter extremities of  $G_\alpha$  and  $G_\gamma$  subunits including the three lipid-modified  $G_\alpha$ -Gly2,  $G_\alpha$ -Cys3, and  $G_\gamma$ -Cys68. CHARMM parameters for these modified amino acids were built using the CHARMM general force field<sup>14</sup> and the ParamChem webtool (<https://www.paramchem.org/>). The whole protein was then placed in the proximity of a membrane constituted by 379 1-palmitoyl-2-oleyl-*sn*-glycero-3-phosphocholine (POPC) lipid molecules. The membrane:protein complex was then solvated in each  $z$  direction, resulting in a box size of about  $130 \times 130 \times 150 \text{ \AA}^3$ . Fourteen sodium ions were randomly added to this box to neutralize charges of the whole system finally comprising 214 830 atoms. G-protein orientation to the membrane was performed in agreement with the recent crystallographic structure describing the G-protein: $\beta 2$ -adrenergic receptor

complex.<sup>6</sup> The Particle Mesh Ewald (PME) method was used for computation of electrostatic interactions. The Van Der Waals interactions were truncated at 12 Å through the use of a switching function applied in the range 10:12 Å. The NPT ensemble was used (1.013 bar and 298 K) with Langevin dynamics and a Nosé–Hoover Langevin piston pressure control. The integration step was set to 1 fs. The Interactive Molecular Dynamics (IMD) protocol was used as implemented in NAMD and VMD,<sup>15</sup> to slowly insert the anchoring residues into the membrane. During this step, only residues localized around the protein anchoring points were allowed to move, all the others being constrained at their initial positions. The obtained configuration was then energy-minimized through 5,000 steps of conjugate gradient to avoid steric clashes and then submitted to a first 2 ns MD simulation during which all the protein atoms were kept fixed. In a second stage, all constraints were removed, and new velocities were assigned. The simulation was finally stopped after 90 ns.

**Targeted Molecular Dynamics Simulations.** Starting from the conformation obtained after 30 ns of MD trajectory, we then ran three independent 20 ns Targeted Molecular Dynamics (TMD)<sup>16</sup> simulations. The same parameters as those used in the initial MD were used, except for the random seed number that was changed to generate different sets of initial velocities. No constraint was applied during the first 4 ns of each TMD run to assume correct re-equilibration of the system. The crystallographic structure (PDB code: 1GIA)<sup>7</sup> describing the active state of the  $G_{i\alpha}$  subunit complexed to GTP was used as a target position. Only backbone atoms of residues 34 to 343 of  $G_{i\alpha}$  were submitted to the TMD constraint. This allowed us

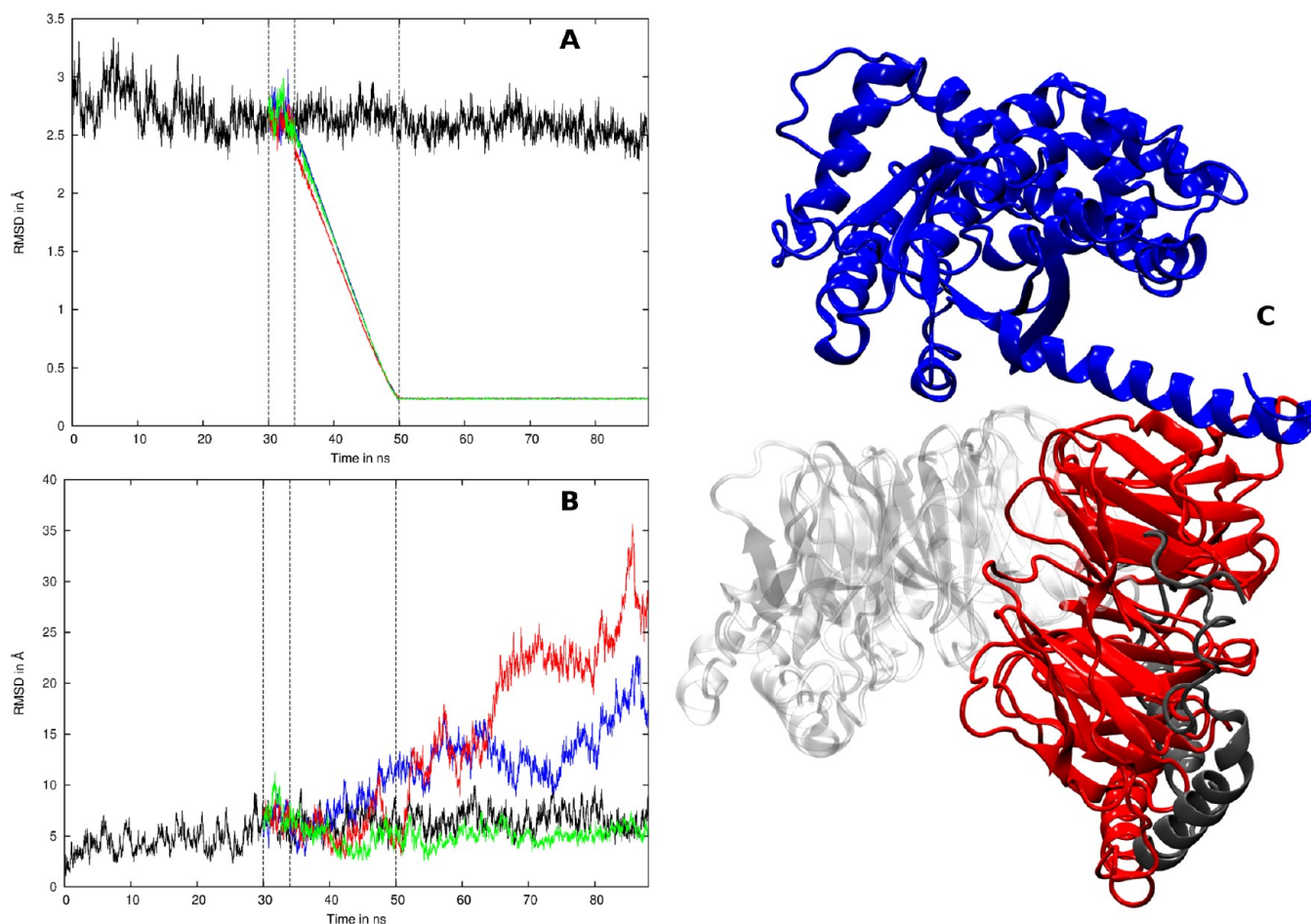


**Figure 2.** (A) RMSD values computed against the target ( $G_{\alpha}$  subunit) for each of the three TMD runs and including 30 ns of unconstrained MD, 4 ns of re-equilibration, 16 ns of TMD, and 38 ns of additional MD with the  $G_{\alpha}$  subunit constrained to the target. (B) RMSD values computed for the  $G_{\beta\gamma}$  subunit after structural fit on  $G_{\alpha}$  for the same simulation steps showing large motions of  $G_{\beta\gamma}$ . (C) Upper view of the  $G_{\alpha\beta\gamma}$  heterotrimer at the end of the red MD trajectory with the final and the initial positions of the two  $G_{\beta\gamma}$  subunits reported in red and in transparent white, respectively.

to simulate the conformational transition from the inactive (GDP bound) to the active (GTP bound) states of  $G_{\alpha}$  by applying a force to each constrained atom of the system that was of the form

$$\vec{F}(t) = \frac{1}{2}k(\text{RMSD}_{\text{obs}}(t) - \text{RMSD}_{\text{targ}}(t))^2 \quad (1)$$

where  $k$  is a force constant of  $10 \text{ kcal mol}^{-1} \text{ \AA}^{-2}$  and  $\text{RMSD}_{\text{obs}}(t)$  and  $\text{RMSD}_{\text{targ}}(t)$  are the observed and targeted values of the Root Mean Square Deviation (RMSD) at a given time step  $t$ , respectively. RMSDs were computed on the entire set of constrained atoms.

After having verified the success of the transition between  $G_{\alpha}$  subunit inactive and active conformations, the TMD forces were conserved to maintain the  $G_{\alpha}$  subunit in its active conformation for 38 ns of additional simulation.

To resume, each “TMD run” finally comprised 58 ns of MD divided into three successive stages: (i) a 4 ns re-equilibration of the system, (ii) a 16 ns pulling step of  $G_{\alpha}$  from its inactive to its active conformations, and (iii) the last 38 ns stage in which  $G_{\alpha}$  was forced to keep its active conformation.

## RESULTS

As an initial step of this study, we first built a  $G_{\alpha\beta\gamma}$ :GTP complex in the «inactive» conformation by replacing the

GDP by a GTP molecule in the X-ray structure available for the  $G_{\alpha\beta\gamma}$ :GDP complex (PDB code: 1GP2).<sup>10</sup> As expected from X-ray structures (see Figure 1B), this replacement did not cause any particular steric clash. This model was further anchored to the membrane by lipid-modified residues, as previously described,<sup>17</sup> and equilibrated in a first 90 ns unconstrained molecular dynamics simulation. By this, we simulated a complex, the structure of which had not been experimentally solved, that mimicked the immediate following step after GTP entrance in its dedicated pocket.

Starting from the conformation obtained at 30 ns, the  $G_{\alpha}$  subunit was further constrained to evolve from its inactive (GDP bound) to its active (GTP bound) conformation, assuming that conformational rearrangements observed in available X-ray structures were due to the presence of the GTP.<sup>18</sup> Because of the complexity of these changes (see Figure 1A), including the formation of two additional helix turns in switches II and IV, and a concerted motion of the switch III, that could hardly be simulated by other unbiased methods, the targeted MD method was used. In our calculations, only the backbone atoms of the  $G_{\alpha}$  subunit were subjected to the TMD constraint, so that the resulting conformational changes on the whole heterotrimer could be observed and discussed. Importantly, side-chains of all residues were also free to move, allowing one to observe and discuss local conformational



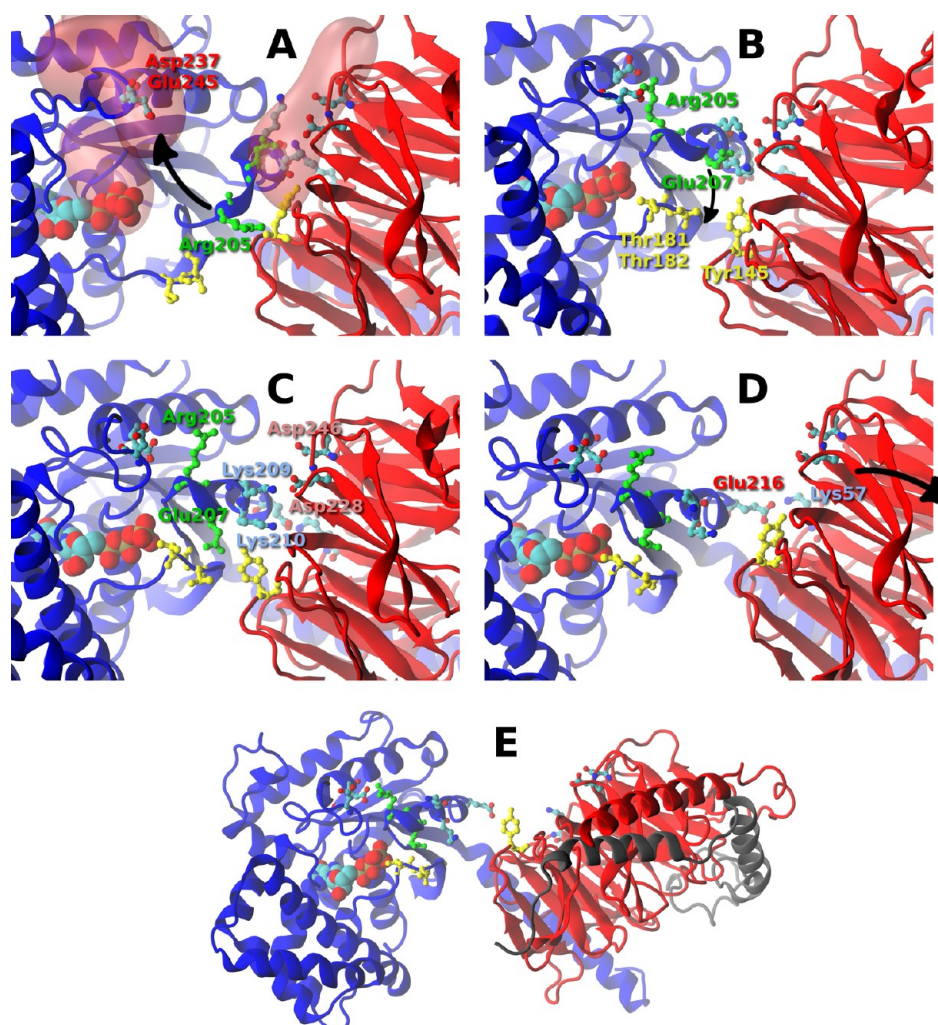


**Figure 3.** Putative dissociation mechanism of  $G_\alpha$  and  $G_{\beta\gamma}$  after GTP entrance in the  $G_\alpha$  subunit. This involved the successive rotations of Arg205 and Glu207 and the break of interactions at the interface of both subunits. Water, ions, and lipid molecules were removed from the figure.

rearrangements as well. These calculations were performed three times, starting from the same conformation at 30 ns of the initial MD trajectory but changing the initial velocities to verify the robustness of the data.

In all three TMD simulations, the  $G_\alpha$  subunit successfully evolved from its inactive to its active conformation, as shown by the RMSD curves reported in Figure 2A and showing RMSD < 0.25 Å to the target after 50 ns. Interestingly, it was observed that the imposed local conformational changes of the  $G_\alpha$  subunit allowed a large reorientation of  $G_{\beta\gamma}$ , which behaved as a rigid block. Indeed, RMSDs reported in Figure 2B and reaching 30 Å in one of the three trajectories resulted in large motions of  $G_{\beta\gamma}$  in respect to  $G_\alpha$ . Such a behavior was observed in two of the three TMD runs (red and blue curves). Such RMSD values reflected the almost total dissociation of the heterotrimeric G-protein as reported in Figure 2C. This dissociation was characterized by a rotation of about 50° of the block formed by both the  $G_\alpha$  N-terminal helix and  $G_{\beta\gamma}$  subunits. Surprisingly, the  $C_\alpha$  fluctuations of  $G_{\beta\gamma}$  did not change during the separation of these two blocks, suggesting that dissociation of the G-protein did not require any intrinsic  $G_{\beta\gamma}$  rearrangement. This was confirmed by the computation and the comparison of the Root Mean Square Fluctuations (RMSFs) of each residue of the protein either during the unconstrained MD

simulation of 90 ns or during each of the three TMD simulations. The results of this analysis are reported in Figure S11 and confirm that, even during the TMDs, no important conformational change was observed for such a protein domain (SCOP classification) showing a low degree of flexibility (data not shown). As a method validation, the simulation in which the separation was not observed (green) confirmed the transition speed between both  $G_\alpha$  states was sufficiently low to allow  $G_{\beta\gamma}$  (i) to relax on such a time-scale and (ii) to follow the  $G_\alpha$  transition. Thus, it could be confirmed here that the observed dissociation was effectively due to the conformational changes occurring in  $G_\alpha$  and not to a putative bias of the TMD method.

**Putative Molecular Mechanism for G-Protein Dissociation.** Taking advantage of our all-atom simulations, we were further interested in understanding how an additional phosphate in GTP could promote the breaking of interactions at the interface between  $G_\alpha$  and  $G_{\beta\gamma}$ . After having computed the electrostatic potential of the GTP bound protein after 30 ns of trajectory, it was observed that the presence of the third phosphate resulted in a highly negatively charged pocket, which was represented in Figure 3A. Analysis of the three TMD runs

showed that Arg205 was the sole positively charged residue, reorienting significantly in this pocket (Figure 3A,B). This reorientation of the side-chain of Arg205 contributed to form a cluster of hydroxylated residues in the same region (yellow residues, Figure 3B) and comprising residues Thr181, Thr182, and Tyr145. Interestingly, this cluster was at the origin of the reorientation of a second positively charged residue, Glu207 (Figure 3B,C), thus destabilizing the ionic cluster localized at the interface of  $G_\alpha$  and  $G_{\beta\gamma}$  and involving Lys209 and Lys210 of  $G_\alpha$  with Asp228 and Asp246 of  $G_\beta$  (Figure 3C). Breaking of these interactions initiated the separation of the two subunits (Figure 3D). On a longer time-scale, another break of ionic interaction occurred and involved Glu207 and Lys57 (Figure 3D), thus finalizing full separation of the two blocks (Figure 3E). In the “green” simulation (see Figure 2) in which the separation of the two  $G_\alpha$  and  $G_{\beta\gamma}$  blocks was not observed, the ionic cluster was not totally broken and the protein was trapped in step “D” of Figure 3.

## DISCUSSION

Obviously, many X-ray structures are now available for G-proteins subunits, both in their isolated<sup>7,9,19</sup> and GPCR complexed conformations,<sup>6</sup> their mechanism of dissociation at the molecular level still remaining to be elucidated. This dissociation occurs after the crucial and rate limiting step of GDP:GTP exchange in the  $G_\alpha$  subunit that promotes local conformational changes. In this study, we observed such a molecular dissociation during MD simulations on the 100 ns time-scale. Our results strongly suggested that these local structural rearrangements, that could be deduced from analysis of the available X-ray structures, might be sufficient to promote separation of the  $G_\alpha$  and  $G_{\beta\gamma}$  blocks in the biological membrane proximity. Thanks to our all-atom description, the significance of some residues belonging to both these subunits was highlighted. Site-directed mutagenesis experiments are now in progress to support the involvement of these residues in the G-protein dissociation mechanism.

Nevertheless, it was not excluded that the receptor might have a significant role in this dissociation process. Indeed, no complete dissociation was observed in our simulations; strong interactions between the  $G_{\beta\gamma}$  complex and N-ter helix of  $G_\alpha$  were not broken. The putative motions of the tetrameric complex ( $\beta_2$ -adrenergic receptor +  $G_s$  heterotrimer), analyzed by NMA, were in good agreement with those depicted here. This suggested a synergetic process between GTP binding and motions induced by the protein:protein interactions (under investigation in our laboratory).

In our calculations, we did not include the  $Mg^{2+}$  ion, which appears in most of the available X-ray structure of the  $G_\alpha$ :GTP complex. Indeed, the binding of this positive ion, which is in direct interaction with the third phosphate of GTP is thought to occur after the local structural rearrangements, probably in the isolated  $G_\alpha$  subunit, and after the dissociation step. The presence of the  $Mg^{2+}$  ion is absolutely required for GTP hydrolysis,<sup>20</sup> whereas no experimental data have yet proven its role in the structural stability of the interface between the  $G_\alpha$  and the  $G_{\beta\gamma}$  subunits.

## ASSOCIATED CONTENT

### Supporting Information

Root mean square fluctuations (RMSFs) computed for each residue of the  $G_\alpha$  (A),  $G_\beta$  (B), or  $G_\gamma$  (C) subunits along each of

the obtained trajectories. This material is available free of charge via the Internet at <http://pubs.acs.org>.

## AUTHOR INFORMATION

### Corresponding Author

\*E-mail: [nicolas.floquet@univ-montp1.fr](mailto:nicolas.floquet@univ-montp1.fr).

### Notes

The authors declare no competing financial interest.

## ACKNOWLEDGMENTS

We thank the University Montpellier 1 for Ph.D. and postdoctoral fellows of M.L. and L.C. We thank J. Marie, J. L. Banères, D. Gagne, C. M’Kadmi, J. C. Galleyrand, and J. A. Fehrentz (Institut des BioMolécules Max Mousseron, Centre National de la Recherche Scientifique UMR5247) for constructive remarks. This study was also realized with the support of HPC@LR, a Center of competence in High-Performance Computing from the Languedoc-Roussillon region, funded by the “Région Languedoc-Roussillon”, the Europe and the Université Montpellier 2 Sciences et Techniques. The HPC@LR Center is equipped with an IBM hybrid supercomputer.

## REFERENCES

- (1) Tang, X.; Wang, Y.; Li, D.; Luo, J.; Liu, M. Orphan G protein-coupled receptors (GPCRs): biological functions and potential drug targets. *Acta Pharmacol. Sin.* **2012**, *33*, 363–371.
- (2) Kapoor, N.; Menon, S. T.; Chauhan, R.; Sachdev, P.; Sakmar, T. P. Structural Evidence for a Sequential Release Mechanism for Activation of Heterotrimeric G Proteins. *J. Mol. Biol.* **2009**, *393*, 882–897.
- (3) Mixon, M. B.; Lee, E.; Coleman, D. E.; Berghuis, A. M.; Gilman, A. G.; Sprang, S. R. Tertiary and quaternary structural changes in Gi alpha 1 induced by GTP hydrolysis. *Science* **1995**, *270*, 954–960.
- (4) Morikawa, T.; Muroya, A.; Nakajima, Y.; Tanaka, T.; Hirai, K.; Sugio, S.; Wakamatsu, K.; Kohno, T. Crystallization and preliminary X-ray crystallographic analysis of the receptor-uncoupled mutant of Gai1. *Acta Crystallogr., Sect. F* **2007**, *63*, 139–141.
- (5) Johnston, C. A.; Willard, F. S.; Jezyk, M. R.; Fredericks, Z.; Bodor, E. T.; Jones, M. B.; Blaesius, R.; Watts, V. J.; Harden, T. K.; Sondek, J.; Ramer, J. K.; Siderovski, D. P. Structure of Gai1 Bound to a GDP-Selective Peptide Provides Insight into Guanine Nucleotide Exchange. *Structure* **2005**, *13*, 1069–1080.
- (6) Rasmussen, S. G. F.; DeVree, B. T.; Zou, Y.; Kruse, A. C.; Chung, K. Y.; Kobilka, T. S.; Thian, F. S.; Chae, P. S.; Pardon, E.; Calinski, D.; Mathiesen, J. M.; Shah, S. T. A.; Lyons, J. A.; Caffrey, M.; Gellman, S. H.; Steyaert, J.; Skiniotis, G.; Weis, W. I.; Sunahara, R. K.; Kobilka, B. K. Crystal structure of the  $\beta_2$  adrenergic receptor-Gs protein complex. *Nature* **2011**, *477*, 549–555.
- (7) Coleman, D. E.; Berghuis, A. M.; Lee, E.; Linder, M. E.; Gilman, A. G.; Sprang, S. R. Structures of active conformations of Gi alpha 1 and the mechanism of GTP hydrolysis. *Science* **1994**, *265*, 1405–1412.
- (8) Noel, J. P.; Hamm, H. E.; Sigler, P. B. The 2.2 Å crystal structure of transducin- $\alpha$  complexed with GTP $\gamma$ S. *Nature* **1993**, *366*, 654–663.
- (9) Davis, T. L.; Bonacci, T. M.; Sprang, S. R.; Smrcka, A. V. Structural and Molecular Characterization of a Preferred Protein Interaction Surface on G Protein  $\beta\gamma$  Subunits. *Biochemistry* **2005**, *44*, 10593–10604.
- (10) Wall, M. A.; Coleman, D. E.; Lee, E.; Iñiguez-Lluhi, J. A.; Posner, B. A.; Gilman, A. G.; Sprang, S. R. The structure of the G protein heterotrimer Gi alpha 1 beta 1 gamma 2. *Cell* **1995**, *83*, 1047–1058.
- (11) Phillips, J. C.; Braun, R.; Wang, W.; Gumbart, J.; Tajkhorshid, E.; Villa, E.; Chipot, C.; Skeel, R. D.; Kalé, L.; Schulten, K. Scalable molecular dynamics with NAMD. *J. Comput. Chem.* **2005**, *26*, 1781–1802.

- (12) Feller, S. E.; MacKerell, A. D. An Improved Empirical Potential Energy Function for Molecular Simulations of Phospholipids. *J. Phys. Chem. B* **2000**, *104*, 7510–7515.
- (13) Mackerell, A. D. Empirical force fields for biological macromolecules: Overview and issues. *J. Comput. Chem.* **2004**, *25*, 1584–1604.
- (14) Vanommeslaeghe, K.; Hatcher, E.; Acharya, C.; Kundu, S.; Zhong, S.; Shim, J.; Darian, E.; Guvench, O.; Lopes, P.; Vorobyov, I.; Mackerell, A. D., Jr. CHARMM general force field: A force field for drug like molecules compatible with the CHARMM all atom additive biological force fields. *J. Comput. Chem.* **2010**, *31*, 671–690.
- (15) Humphrey, W.; Dalke, A.; Schulten, K. VMD: visual molecular dynamics. *J. Mol. Graphics* **1996**, *14* (33–38), 27–28.
- (16) Schlitter, J.; Engels, M.; Krüger, P. Targeted molecular dynamics: a new approach for searching pathways of conformational transitions. *J. Mol. Graphics* **1994**, *12*, 84–89.
- (17) Louet, M.; Perahia, D.; Martinez, J.; Floquet, N. A concerted mechanism for opening the GDP binding pocket and release of the nucleotide in hetero-trimeric G-proteins. *J. Mol. Biol.* **2011**, *411*, 298–312.
- (18) Lambright, D. G.; Noel, J. P.; Hamm, H. E.; Sigler, P. B. Structural determinants for activation of the  $\alpha$ -subunit of a heterotrimeric G protein. *Nature* **1994**, *369*, 621–628.
- (19) Sondek, J.; Lambright, D. G.; Noel, J. P.; Hamm, H. E.; Sigler, P. B. GTPase mechanism of Gproteins from the 1.7-Å crystal structure of transducin  $\alpha$ -GDP AIF<sup>4-</sup>. *Nature* **1994**, *372*, 276–279.
- (20) Li, G.; Zhang, X. C. GTP Hydrolysis Mechanism of Ras-like GTPases. *J. Mol. Biol.* **2004**, *340*, 921–932.